(REFEREED RESEARCH)

SO_2 ADSORPTION CAPABILITY OF ACTIVATED CARBON NANOFIBERS PRODUCED BY DIFFERENT ACTIVATION PROCESS PARAMETERS

FARKLI AKTİVASYON PROSES PARAMETRELERİ İLE ÜRETİLEN AKTİVE EDİLMİŞ KARBON NANOLİFLERİN SO_2 ADSORPSİYON ÖZELLİKLERİ

Nuray UCAR[1*], Zeynep CAVDAR[2], Nilgun KARATEPE[3], Pelin ALTAY[1], Nuray KIZILDAG[1]

Istanbul Technical University, Textile Engineering Department, Istanbul, Turkey
[2]Istanbul Technical University, Nano-Science and Nano-Engineering Program, Graduate School of Science, Engineering and Technology, Istanbul, Turkey
[3]Istanbul Technical University, Institute of Energy, Istanbul, Turkey

Received: 08.02.2016 Accepted: 08.11. 2016

ÖZET

Bu çalışmada, aktivasyon süresi (30 dakika ve 60 dakika) ve aktivasyon gaz (CO_2) besleme hızları (100 mL/dak ve 150 mL/dak) değiştirilerek, aktif karbon nanoliflerin, zararlı SO_2 gazını adsorplama özelliği incelenmiştir. FTIR analizinde 1050 cm-1 civarlarında görülen pik ve SEM-EDS elemental analizde tespit edilen S elementi, adsorplamanın gerçekleştiğini göstermektedir. CO_2 besleme hızı azaldıkça ve aktivasyon süresi arttıkça, SO_2 adsorplama miktarının arttığı, her iki parametrenin artması ile aktive olmuş nanolifin lif çapının düştüğü görülmüştür. SO_2 adsorplama kapasitesine tesir bakımından, aktivasyon süresi değişiminin, CO_2 besleme hızı değişiminden daha fazla tesirli olduğu tespit edilmiştir.

Anahtar Kelimeler: Elektroeğirme, karbonizasyon, aktif karbon nanolif, SO_2 adsorplama

ABSTRACT

In this study, the effect of activation time and flow rate of CO_2 on the SO_2 adsorption properties of activated carbon nanofiber has been investigated. The activation process was performed under different CO_2 flow rates (100 and 150 mL/min) and activation times (30 and 60 minutes). At the FTIR spectra, the formation of a new peak at around 1050 cm^{-1} after SO_2 adsorption test, showed the presence of SO_2 adsorbed on the activated carbon nanofibers. The elemental analyses also confirmed the presence of S atom in the analysed sample after SO_2 adsorption test. It has been seen that an increase in activation time and decrease in CO_2 feeding rate resulted in an increase in SO_2 adsorption capability of activated carbon nanofibers. Rather than the flow rate of the activation gas, activation time has higher effect on the SO_2 adsorption capability of activated carbon nanofibers.

Keywords: Electrospinning, carbonization, activated carbon nanofiber, SO_2 adsorption.

Corresponding Author: Nuray Uçar, ucarnu@itu.edu.tr

1. Introduction

Sulphur dioxide (SO_2) is a pollutant which is released in large quantities into the atmosphere, mainly by industries such as oil refineries and automobiles that use fossil fuels. The atmospheric oxidation caused by sulphur dioxide leads to the formation of acid rains, which results in the abrasion of monuments and buildings, an increase in the acidity of soil and water, and the retardation of the development of flora and aquatic life. Besides, SO_2 can react slowly with oxygen to form SO_3, which subsequently reacts with water to form sulfuric acid [1-3]. Several methods have been developed to reduce emissions of SO_2. Activated carbon is a well-known adsorbent because of its capability to remove particulate materials, heavy metals, organic materials, and other air toxics in filtration. They are also reported to be effective in removal of SO_2 from flue gas. Among the

different shapes of activated carbons, activated carbon fiber (ACFs), either at conventional or nanoscale, is one of the most promising adsorbents [3-7].

The activated carbon nanofibers (ACNFs) is a relatively new material compared to activated carbon particles, proposed for use as adsorbent for the removal of volatile organic compounds (VOCs) in filtration and purification systems due to their smaller diameter (sub-micrometer) and more developed micropore structure [8-12]. The production of ACNFs involves precursor nanofiber formation, stabilization of the precursor chemical structure under an oxidizing atmosphere, carbonization under an inert gas, and finally activation under an activating gas, such as CO_2 or water vapour (physical activation) or an oxidizing reagent such as KOH or HNO_3 (chemical activation) [13]. Heat treatment is the most important process for high performance carbon fiber production. The steps of heat treatment also affect the pore sizes of activated carbon fibers in different ranges based on the conditions of processes [14-17]. Activation is carried out to remove the disorganized carbon that blocks the pores in the activated carbon. Apart from this, it can enlarge the diameters of the pores, which are formed during carbonization process and to create some new porosity. Therefore; activation proses leads to a considerable increase in the adsorption capacity, which is mainly due to widening of starting micropores and the development of new micropores [8,11,12,18-21] and also due to the reduction in the volume of mesopores [2]. Activated carbon nanofibers (ACNFs) have excellent properties including lightweight, remarkable mechanical properties, narrower pore size distribution, higher surface area, smaller fiber diameter which minimizes diffusion limitations and allows rapid adsorption and desorption, excellent adsorption capacity at low concentrations, and excellent flexibility [11, 18-24]. They exhibit slit-shaped pores which is the source of its high adsorption capacity [22]. Particularly polyacrylonitrile (PAN)-based ACNFs are reported to show some specific adsorption features for acidic materials owing to a trace of nitrogen atoms contained in their structures [7]. Their performance in adsorption mainly depends on the surface area, pore structure and surface chemistry which are influenced by both the nature of the precursors and the method of activation [25-29].

When literature is reviewed, it has been seen that most of studies performed on activated carbon nanofibers focused on porosity, surface area, and surface chemistry of activated carbon nanofibers [7]. For example, Tavanai et al. (2009) found that the microporosity of ACNFs was more developed than that of ACFs. They examined how the fiber diameter and activation temperature affect the pore characteristics of PAN based activated carbon nanofibers and they demonstrated that the characteristic properties of ACNFs increased by increasing the temperature of activation and decreasing the diameter of fiber [19]. Lee et al. (2013) compared the effects of different activation methods, namely physical (H_2O and CO_2) and chemical (KOH) activation, on pore characteristics and surface area. The specific surface area of the physically ACNFs increased up to 2400 m^2/g and the ACNFs were found to be mainly composed of micropore structures [22]. Ra et al. (2010) used a mixture of camphor and polyacrylonitrile (PAN) to synthesize the carbon nanofibers with high microporosity and high surface area as a result of evaporation of camphor during leaving micropores in the fiber structure [28]. On the other hand, the studies performed on SO_2 adsorption ability of activated carbon nanofibers are very limited. For example, Song et al. (2008) investigated the effect of the activated carbon fibers, activated carbon nanofibers and modified activated carbon nanofibers by a nitrogenated compound on adsorption capacity for SO_2 and reported that modified activated carbon nanofibers showed the highest adsorption capacity for SO_2 [7]. Sullivan et al. (2012) reported the physical, chemical, adsorptive, and adsorption kinetic properties of a recently developed PAN-derived ACNF adsorbent produced by electrospinning and subsequent carbonization and activation by CO_2. ACNFs were reported to show 2-5 times greater SO_2 adsorption capacities in dry nitrogen, compared to commercially available activated carbon fiber cloth (ACFC) and Calgon BPL™ granular activated carbon. Besides they are reported to display adsorption kinetics nearly twice as fast as ACFC and eight times as fast as Calgon BPL™ [24].

In this study, for the first time, the effects of activation time and flow rate of CO_2 on the SO_2 adsorption properties of activated carbon nanofiber have been investigated in order to provide a contribution to the limited literature. The electrospun PAN nanofiber webs were used as the precursor to prepare carbon nanofiber webs through thermal treatments including stabilization, carbonization and activation. Activation process was performed under different CO_2 flow rates (100 and 150 mL/min) and activation times (30 and 60 minutes). The absorption differences between untreated nanofiber, stabilized nanofiber and activated carbon nanofiber have been examined through SO2-breakthough ratio. The absorption differences among activated carbon nanofibers have been examined through adsorption/desorption/titration method

2. Experimental

2.1 Materials

Polyacrylonitrile was obtained from Sigma Aldrich to use as precursor of carbon nanofiber webs. *N,N'*-Dimethylformamide (DMF) was purchased from Merck Company. Nitrogen was used as inert gas during the carbonization and carbon dioxide gas was used during activation.

2.2 Electrospinning

Polyacrylonitrile (PAN) fiber was first dissolved in *N,N*'-Dimethylformamide to prepare a 15 wt.% solution. The electrospinning was conducted horizontally onto a rotating drum collector with a flow rate of 1.0 mL/hr, an applied voltage of 15 kV and a spinning distance of 10 cm. The experimental set-up used for electrospinning is schematically shown in Figure 1.

2.3 Stabilization, carbonization and CO_2 activation

Electrospun nanowebs were subjected to stabilization, carbonization and activation processes. The electrospun

fiber web was firstly stabilized in PROTHERM PLF series chamber furnace at 245ºC for 1 hour at a heating rate of 1ºC/min under the air flow. Activation and carbonization processes were performed by using PROTHERM PTF series tube furnace. The stabilized nanofiber bundle was subsequently carbonized at 800ºC in an inert (high purity nitrogen gas) environment with the heating rate set at 5ºC/min. The temperature of furnace was kept at the same temperature to achieve the activation under CO_2 atmosphere at a flow rate of 100 mL/min and 150 mL/min for 30 and 150 mL/min for 60 minutes. The samples produced are listed in Table 1.

2.4 Characterization

Morphological and Elemental Analysis (SEM-EDS)

Scanning Electron Microscopy with Energy Dispersive Detector (Philips FEI - Quanta FEG 250) was used to observe the surface morphology of the samples and to determine the elements present in the samples. The samples were firstly sputter coated with Au-Pd using Quorum - SC7620 Sputter Coater.

Fourier Transform Infra-Red Spectroscopy (FTIR)

Fourier transform infrared (FTIR) absorption spectra for PAN150CO_2-60min sample before and after SO_2 adsorption were taken with Perkin Elmer spectrometer to confirm the SO_2 adsorption by the sample. The scanning ranged from 4000 cm^{-1} to 400 cm^{-1}.

SO_2 adsorption test system and monitoring the SO_2–breakthrough ratio

The SO_2 adsorption capabilities of the samples were measured using an experimental setup, the schematic diagram of which is presented in Figure 2.

A certain amount of sample (with a diameter of 2.38 cm) was placed vertical to the gas stream in the quartz reactor which is located in the tube furnace and a gas mixture containing SO_2 was introduced into the reactor. SO_2 gas was fed with pure nitrogen for 60 min. The flow rates of the N_2 and SO_2 gas streams were kept at 150 mL/min and 1.47 mL/min, respectively. The SO_2 concentration was monitored and recorded on a SO_2 single gas detector (TESTO350 Easy Emission) at 1 s intervals.

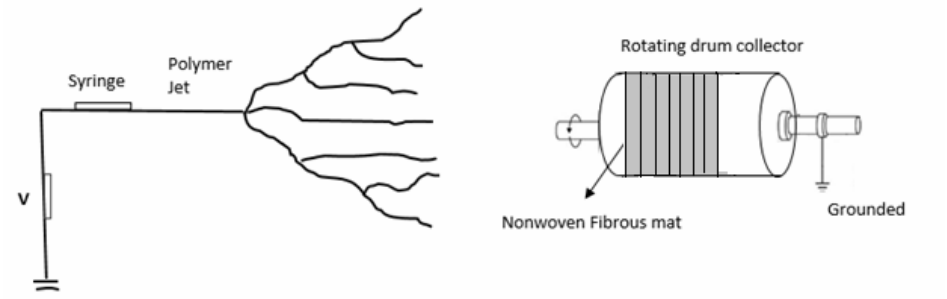

Figure 1. Schematic of electrospinning setup.

Table1. Samples produced and the process conditions used.

Sample code	Process conditions
PAN	Untreated sample
PAN-stab	24 h stabilized at 245°C
PAN100CO_2-30min	Carbonized at 800°C with the heating rate of 5 °C/min, Activation with CO_2 at a flow rate of 100 mL/min for 30 min
PAN150CO_2-30min	Carbonized at 800°C with the heating rate of 5 °C/min, Activation with CO_2 at a flow rate of 150 mL/min for30 min
PAN150CO_2-60min	Carbonized at 800°C with the heating rate of 5 °C/min, Activation with CO_2 at a flow rate of 150 mL/min for 60 min

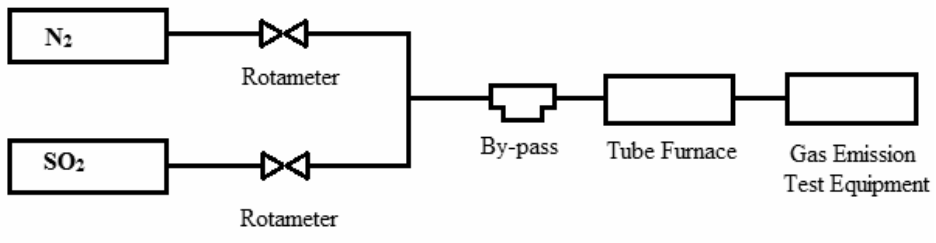

Figure 2. Schematic diagram of the experimental setup for SO_2 adsorption.

The adsorption ratio was calculated using the below formula;

SO_2breakthrough ratio = *C/Co* (1)

where; Co and C were inlet SO_2 concentration and outlet SO_2 concentration measured by gas detector during adsorption test, respectively. When C/Co is equal to 1, it means that no adsorption took place and all the SO_2 passed through the tube without being adsorbed onto the samples. Co is constant and it is measured as 1470 ppm.

Investigation of SO_2 adsorption capability by desorption and titration method

This method consisted of three different steps, namely adsorption, desorption and titration. SO_2 adsorption was performed following the procedures described in the previous section using the setup shown in Figure 2. During adsorption test, SO_2 was fed with N_2 in order to be able to set the concentration of SO_2. For desorption and titration, the experimental setup which is illustrated in Figure 3 is used.

The desorption step was carried out in the same furnace at the temperature of 360°C. For desorption, the samples, which were exposed to SO_2 adsorption analysis, were heated to 360 ºC in the tube furnace at a heating rate of 5 ºC/min and the temperature was kept constant for 60 min. During the desorption step, the outlet gas (SO_2 adsorbed by the samples) was all bubbled within a solution containing 5% H_2O_2. The desorbed SO_2 was supposed to form H_2SO_4 when the outlet gas was passing through H_2O_2 solution. When the desorption process was finished, this solution containing H_2SO_4 was analyzed by titration method which used 0.1 N NaOH and bromfenol blue as indicator. The amount of SO_2 adsorbed by the activated carbon nanofibers for a given adsorption condition was then evaluated.

Results and Discussion

3.1 Scanning Electron Microscopy (SEM)

SEM images of the samples are shown in Figure 4 and the average nanofiber diameters are given in Table 2.

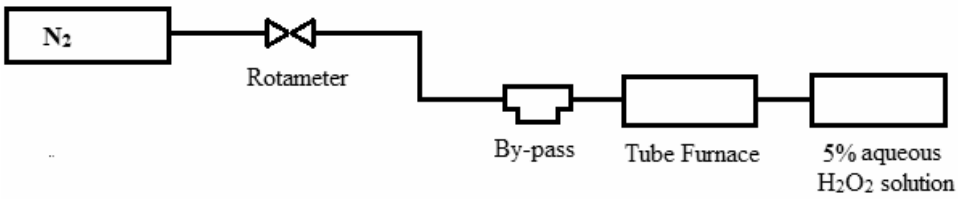

Figure 3. Schematic diagram of the experimental setup for SO_2desorption and titration.

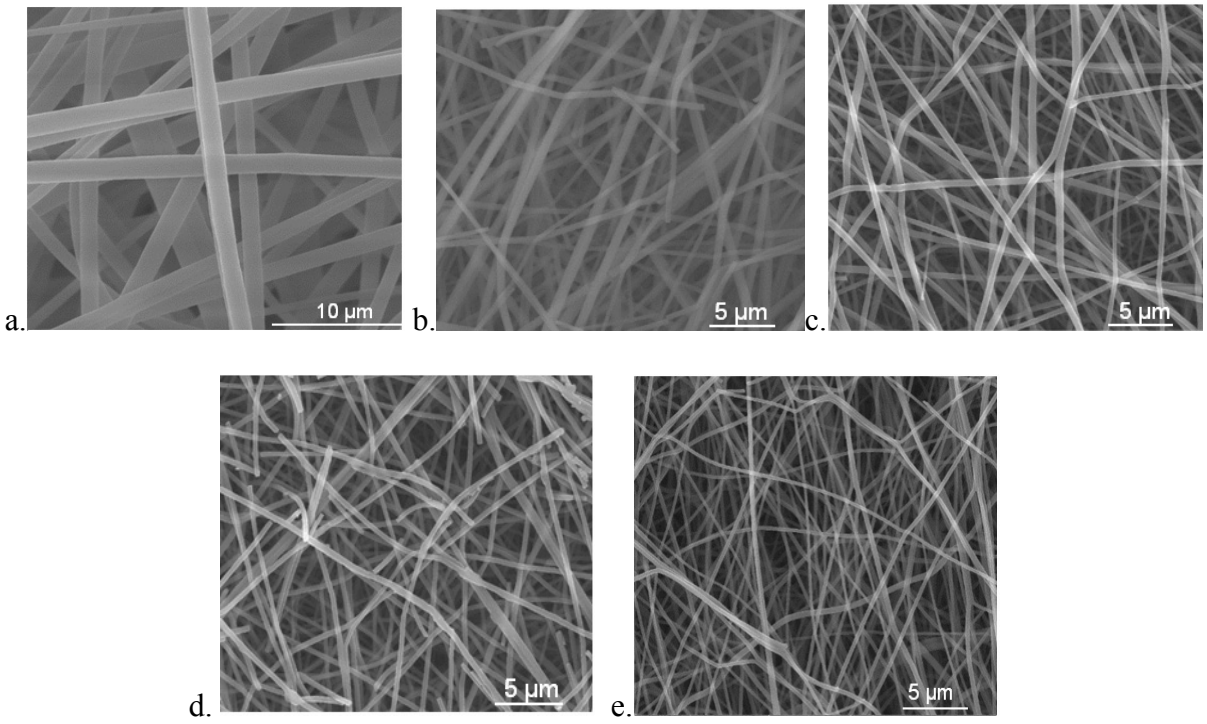

Figure 4. SEM images of a. PAN; b. PAN-stab; c. PAN100CO_2-30min; d. PAN150CO_2-30min; e. PAN150CO_2-60min

From the data presented in Table 2 and Figure 4, it was observed that the average nanofiber diameter reduced after carbonization as compared to the untreated and stabilized PAN nanofiber. It is reported in literature that, during carbonization, a variety of gases (e.g., H_2O, N_2, HCN, and others) evolves as a result of which significant loss in the weight of ACNFs occurs leading to the reduction in fiber diameter [8,18,30,31]. Thus; the reduction observed in average nanofiber diameter during carbonization can be attributed to the formation of more compact structure by dehydrogenation, deoxygenation, and denitrogenation from the precursor [12]. From the data presented in Table 2 and Figure 4, it was also observed that the average diameter of carbonized samples decreased as the CO_2 flow rate and process time increased.

Table 2. Average diameters of nanofibers.

Samples	Average nanofiber diameter (nm) ± standard deviation
PAN	1447.6 ± 259.9
PAN-stab	778.8 ± 147.9
PAN100CO_2-30min	515.3 ± 119.8
PAN150CO_2-30min	429.3 ± 53.3
PAN150CO_2-60min	324.6 ± 97.3

3.2 FTIR

Fourier transform infrared (FTIR) absorption spectra for PAN150CO_2-60min sample before and after SO_2 analysis are presented in Figure 5.

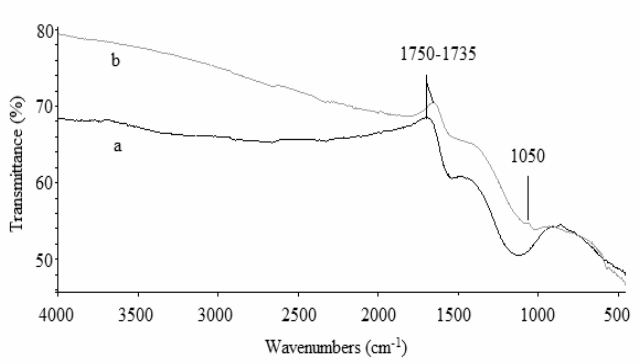

Figure 5. FTIR spectra of PAN150CO_2-60min a. before SO_2 analysis; b. after SO_2 analysis.

The characteristic vibrational frequencies associated with SO*x* are as follows: SO*x* stretching vibrations, 950–1250 cm^{-1}; SO*x* angle deformation vibrations, 500–700 cm^{-1} [32]. The formation of a new peak at around 1050 cm^{-1} after SO_2 adsorption test, showed the presence of SO_2 adsorped on the activated carbon nanofibers. In the literature, the 1540-1800 cm^{-1} band was assigned to the C=O streching mode in carbonyls, carboxylic acids and lactones, whereas the 1000-1440 cm^{-1} band was assigned to the C-O stretching and O-H bending in phenols and carboxylic acids [33].

3.3 Elemental Analysis (SEM-EDS)

Elemental analysis was performed for PAN150CO_2-60min sample before and after SO_2 adsorbance. The EDS spectra obtained are presented in Figure 6 and the weight percentages of the elements are presented in Table 3. While the peaks of the sample before SO_2 adsorbance corresponded to the C, N and O atoms, a new distinctive peak corresponding to S atom appeared after SO_2 adsorbance which confirmed that SO_2 was adsorbed on the activated carbon nanofiber samples. The elemental analysis (Figure 6 and Table 3) confirmed the presence of S atom in the analysed sample. For PAN150CO_2-60min sample, the percentage of K counts for S atom was measured as 4.19 % after SO_2 adsorbance.

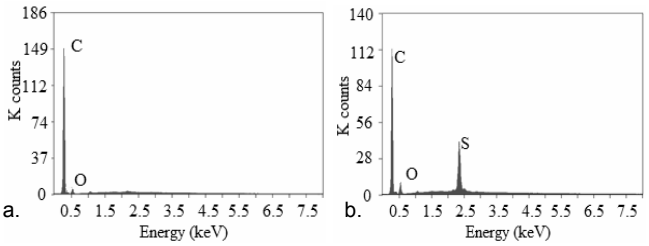

Figure 6. EDS spectra of PAN150CO_2-60min a. before SO_2 adsorbance; b. after SO_2 adsorbance.

Table 3. Elemental analysis of PAN150CO_2-60min before and after SO_2 adsorbance.

Element	Weight % (Before SO_2 adsorption)	Weight % (After SO_2 adsorption)
C	80.15	76.08
N	10.98	9.30
O	8.87	10.44
S	-	4.19

3.4 Analysis of SO_2 adsorption capability through SO_2–breakthrough ratio

Samples were subjected to SO_2 carried by N_2 at room temperature. SO_2 is expected to be adsorbed onto free sites on fiber surfaces where they are oxidized to sulphur trioxide. The adsorption capacity of a porous carbon material is determined mainly by the pore structure, surface area and the presence of functional groups on the adsorbent [34].

The SO_2 adsorption capabilities of the samples were measured following the procedures explained in the experimental section and the resulting breakthrough profiles are presented in Figures 7 and 8. While Figure 7 enables to compare the effect of gas flow rate on SO_2 adsorption capability, Figure 8 shows the breakthrough profiles of the samples which were exposed to the activation gas (CO_2) for different times as 30 min and 60 min.

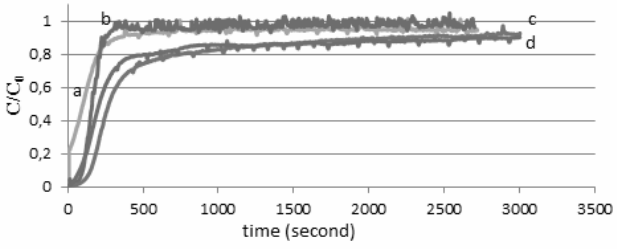

Figure 7. Breakthrough curves of SO_2 for a. PAN (untreated), b. PAN stab; c. PAN100CO_2-30min; d. PAN150CO_2-30 min samples.

In Figure 7 and Figure 8, both PAN (untreated) and the stabilized sample seems to have reached saturation (nearly C/C_0=1) in a very short time of around 200s-400s. Activation with CO_2 results in the formation of well-structured micropores and mesopores in nanofiber structure and increase in the specific surface area which leads to the development of adsorption ability [22].Thus, activated carbon nanofiber has a clear adsorption capability compared to stabilized samples. When the breakthrough profiles of the samples, which were activated physically by CO_2 fed at different rates of 100 mL/min and 150 mL/min (PAN100CO_2-30min and PAN150CO_2-30 min) were compared**,** PAN150CO_2-30 min showed slightly higher adsorption ability (lower C/C_0 values) in the first 500s-1000s. After 1300 s, PAN100CO_2-30 min showed a slightly higher adsorption than PAN150CO_2-30 min. Since both of graphs are very near each other and opposite behaviour with slight differences is available for before and after 1300 s, it is difficult to decide on the effect of flow rate on adsorption capacity by using just only breakthrough profiles without making titration test. Thus, by using breakthrough profiles, it can be possible to point out an improvement on adsorption capacity of activated samples compared to stabilized sample, but the effect of flow rate on adsorption capacity should be evaluated together with titration result given in Section 3.5.

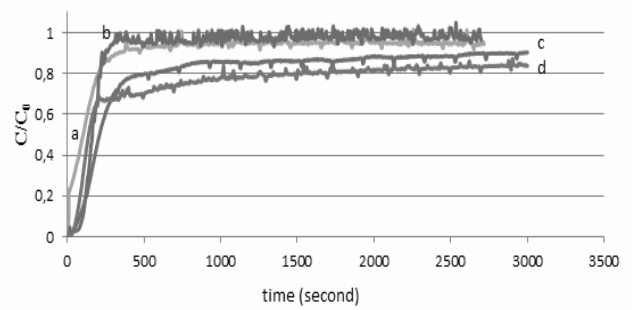

Figure 8. Breakthrough curves of SO_2 for a. PAN (untreated), b. PAN stab; c. PAN150CO_2-30min; d. PAN150CO_2-60min samples.

According to Figure 8, while in first 100s-300s, PAN150CO_2-60min sample has a higher adsorption, after this point, PAN150CO_2-60min sample has a higher adsorption than that of PAN150CO_2-30min sample. It is difficult to decide on the effect of time on adsorption capacity by just only breakthrough profiles without making titration test. Thus it can be possible to point out an improvement on adsorption capacity of activated samples compared to stabilized sample by using breakthrough profiles, but the effect of time on adsorption capacity should be evaluated together with titration result given in Section 3.5.

3.5 Analysis of SO_2 adsorption capability through adsorption, desorption and titration method.

The amounts of SO_2 measured as a result of adsorption, desorption and titration for different samples are presented in Table 4.

Table 4. SO_2 amounts adsorbed by activated carbon nanofibers.

Samples	SO_2 amount adsorbed onto the sample (mg/g sorbent)
PAN100CO_2-30min	329.7
PAN150CO_2-30min	262.6
PAN150CO_2-60min	640.0

Based on titration method (Table 4), PAN100CO_2-30min 100 mL/min showed higher adsorption than PAN150CO_2-30min**.** According to Bhati et al. [27], an increase in flow rate (from 100 mL/min to 400 mL/min) results in increases in surface area, total pore volume, micropore volume, mesopore volume and average pore diameter and decrease in microporosity. The increase in the average pore diameter, total pore volume, micropore volume and mesopore volume and decrease in microporosity means that the number of micropores, where the adsorption mainly occurs, decreased with the increase in the flow rate. Thus, this might have resulted in lower SO_2 adsorption for higher CO_2 feeding rate. According to Table 4, it is possible to say an activation time had higher effect on the SO_2 adsorption capability of activated carbon nanofibers than the flow rate**.**

CONCLUSIONS

Following results have been concluded for activated carbon nanofibers prepared with different activation time and CO_2 feeding rate:

- The average diameter of carbonized samples decreased as the CO_2 flow rate and activation time increased.
- As the CO_2 feeding rate increased from 100 mL/min to 150 mL/min, the SO_2 adsorption capability decreased.
- As the activation time increased from 30 minute to 60 minute, the SO_2 adsorption capability increased.

According to this study, it can be concluded that rather than the flow rate of the activation gas, activation time has higher effect on the SO_2 adsorption capability of activated carbon nanofibers. Thus, lower flow rate with higher activation time can be suggested for higher adsorption capacity.

ACKNOWLEDGEMENT

This study has been funded by BAP 38332.

REFERENCES

1. Lu, G.Q., Do, D.D., 1991, “Preparation of Economical Sorbents for SO_2 and NOx Removal Using Coal Washery Reject”, *Carbon,* 29, 207–213.
2. Plens, A.C.O., Monaro, D.L.G., Coutinho, A.R., 2015, “Adsorption of SO_X and NO_X in Activated Viscose Fibers”, *Anais da Academia Brasileira de Ciências,* 87 (2), 1149–1160.
3. Bagreev, A., Bashkova, S., Bandosz, T.J., 2002, “Adsorption of SO_2 on Activated Carbons: The Effect of Nitrogen Functionality and Pore Sizes”, *Langmuir*, 18, 1257–1264.

4. Liu, W., Adanur, S., 2015, “Desulfurization Properties of Modified Activated Carbon Fibers and Activated Carbon Fiber Paper”, *Journal of Industrial Textiles*, 44(4), 513–525.
5. Liu, W., Adanur, S., 2014, “Desulfurization Properties of Activated Carbon Fibers, Journal of Engineered Fibers and Fabrics”, 9(2), 70–75.
6. Mochida, I., Miyamoto, S., Kuroda, K., Kawano, S., Yatsunami, S., Korai, Y., Yasutake, A., Yoshikawa, M., 1999, “Adsorption and Adsorbed Species of SO_2 During Its Oxidative Removal over Pitch-Based Activated Carbon Fibers”, *Energy & Fuels*, 13(2), 369–73.
7. Song, X., Wang, Z., Li, Z., Wang, C., 2008, “Ultrafine Porous Carbon Fibers for SO_2 Adsorption via Electrospinning of Polyacrylonitrile Solution”, *Journal of Colloid and Interface Science,* 327, 388–392.
8. Cuervo, M.R., Asedegbega-Nieto, E., Diaz, E., Vega, A., Ordonez, S., Castillejos-Lopez, E., Rodriguez-Ramos, I., 2008, “Effect of Carbon Nanofiber Functionalization on the Adsorption Properties of Volatile Organic Compounds”, *Journal of Chromatography A,* 1188(2), 264–273.
9. Ramos, M.E., Bonelli, P.R., Cukierman, A.L., Carrott, M., Carrott, P.J.M., 2010, “Adsorption of Volatile Organic Compounds onto Activated Carbon Cloths Cerived from a Novel Regenerated Cellulosic Precursor”, *Journal of Hazardous Materials,* 177(1–3), 175–182.
10. Shim, W.G., Kim, C., Lee, J.W., Yun, J.J., Jeong, Y.I., Moon, H., Yang, K.S., 2006, “Adsorption Characteristics of Benzene on Electrospun-derived Porous Carbon Nanofibers”, *Journal of Applied Polymer Science,* 102(3), 2454–2462.
11. Hsieh, C.T., Chou, Y.W., 2006, “Fabrication and vapor-phase Adsorption Characterization of Acetone and n-hexane onto Carbon Nanofibers”, *Separation Science and Technology,* 41(14), 3155–3168.
12. Lee, K.J., Shiratori, N., Lee, G.H., Miyawaki, J., Mochida, I., Yoon, S.H., Jang, J., 2010, “Activated Carbon Nanofiber Produced from Electrospun Polyacrylonitrile Nanofiber as a Highly Efficient Formaldehyde Adsorbent”, *Carbon,* 48(15), 4248–4255.
13. Nabais, J.M.V, Canario, T., Carrott, P.J.M, Carrott, R.M.M.L., 2007, “Production of Activated Carbon Cloth with Controlled Structure and Porosity from a New Precursor”, *Journal of Porous Materials,* 14, 181–190.
14. Wiles, K.B., 2002, “Determination of Reactivity Ratios for Acrylonitrile/methyl acrylate Radical Copolymerization via Nonlinear Methodologies Using Real Time FTIR”, *MSc thesis*, Faculty of the Virginia Polytechnic Institute and State University: Blacksburg, Virginia.
15. Schwartz, M., 2002, “Encyclopedia of materials, parts, and finishes”, 2nd ed. Boca Raton, Florida: *CRC Press.*
16. Song, Y., Qiao, W., Yoon, S.H., Mochida, I., Guo, Q., Liu, L., 2007, “Removal of formaldehyde at low concentration using various activated carbon fibers”, *Journal of Applied Polymer Science,* 106(4), 2151–2157.
17. Cho, C.W., Cho, D., Ko, Y., Kwon, O.H., Kang, I., 2007, “Stabilization, Carbonization, and Characterization of PAN Precursor Webs Processed by Electrospinning Technique”, *Carbon Letters*, 8(4), 313–320.
18. Barranco, V., Lillo-Rodenas, M.A., Linares-Solano, A., Oya, A., Pico, F., Ibanez, J., Agullo-Rueda, F., Amarilla, J. M., Rojo, J.M., 2010, “Amorphous Carbon Nanofibers and Their Activated Carbon Nanofibers as Supercapacitor Electrodes”, *The Journal of Physical Chemistry C*, 114, 10302–10307.
19. Tavanai, H., Jalili, R., Morshed, M., 2009, “Effects of fiber diameter and CO_2 activation temperature on the pore characteristics of polyacrylonitrile based activated carbon nanofibers”, *Surface and Interface Analysis*, 41, 814–819.
20. Feng, L., Xie, N., Zhong, J., 2014, “Carbon Nanofibers and Their Composites: A Review of Synthesizing, Properties and Applications”, *Materials*, *7*, 3919–3945.
21. Kim, B.H., Bui, N.N., Yang, K.S., Cruz, M.E, Ferraris, J.P.,2009, “Electrochemical Properties of Activated Polyacrylonitrile/pitch Carbon Fibers Produced Using Electrospinning”, *Bulletin of the Korean Chemical Society*, 30(9), 1967–1972.
22. Lee, H.M., Kang, H.R., An, KH., Kim, H.G., Kim, B.J., 2013, “Comparative studies of porous carbon nanofibers by various activation methods”, Carbon Letters, 14(3), 180–185.
23. Wu, Y., Bi, J., Lou, T., Song, T., Yu, H., 2015, “Preparation of a novel PAN/cellulose acetate-Ag based activated carbon nanofiber and its adsorption performance for low-concentration SO_2”, *International Journal of Minerals, Metallurgy and Materials*, 22(4),437–445.
24. Sullivan, P., Moate, J., Stone, B., Atkinson, J.D., Hashisho, Z., Rood, M.J., 2012, “Physical and chemical properties of PAN-derived electrospun activated carbon nanofibers and their potential for use as an adsorbent for toxic industrial chemicals”, *Adsorption*, 18, 265–274.
25. Qin, Y., Wang, Y., Wang, H., Gao, J., Qu, Z., 2013, “Effect of morphology and pore structure of SBA-15 on toluene dynamic adsorption/desorption performance”, *Procedia Environmental Sciences*, 18, 366–371.
26. Billemont, P., Coasne, B., De Weireld, G., 2013, “Adsorption of carbon dioxide, methane, and their mixtures in porous carbons: effect of surface chemistry, water content, and pore disorder”, *Langmuir*, 29, 3328–3338.
27. Bhati, S., Mahur, J.S., Dixit, S., Choubey, O.N., 2013, “Surface and adsorption properties of activated carbon fabric prepared from cellulosic polymer: mixed activation method”, *Bulletin of the Korean Chemical Society*, 34, 569–573.
28. Ra, E.J., Kim T.H., Yu, W.J., An, K.H., Lee, Y.H., 2010, “Ultramicropore formation in PAN/camphor-based carbon nanofiber paper”, Chemical Communications, 46, 1320–1322.
29. Bai, B.C.,Kim, J.G., Im, J.S., Jung, S.C., Lee, Y.S., 2011, “Influence of oxyfluorination on activated carbon nanofibers for CO_2 storage”, Carbon Letters, 12(4), 236–242.
30. Mao, X., Hatton, T.A., Rutledge, G.C., 2013, “A Review of Electrospun Carbon Fibers as Electrode Materials for Energy Storage” Current Organic Chemsitry, 17(13), 1390–1401.
31. Cloirec, P., Brasquet, C., Subrenat, E., 1997, “Adsorption onto fibrous activated carbon: applications to water treatment”, *Energy & Fuels*, 11(2), 331–336.
32. Colthup, N.S., Daly L.H., Wiberly S.E., 1964, “Introduction to Infrared and Raman Spectroscopy”, *Academic Press, New York*, *USA*.
33. Monah, D., Sinqh, KP., Sinqh, V.K., 2005, “Removal of hexavalent chromium from aqueous solution using low-cost activated carbons derived from agricultural waste materials and activated carbon fabric cloth*”, Ind. Eng. Chem. Res*.,44(4):1027-42
34. Bai,B.C., Kim, J.G., Im, J.S., Jung, S.C., Lee, Y.S., 2011, “Influence of oxyfluorination on activated carbon nanofibers for CO2 storage”, *Carbon Letters*, 12(4), 236–242.